

CONTRIBUTED PAPERS

INTENSITY RATIO OF TRANSITION-METAL $L\alpha$ AND $L\beta$ LINES

JUN KAWAI

Department of Materials Science and Engineering, Kyoto University, Sakyo-ku, Kyoto 606-8501, Japan

Chemical effects on the intensity ratio of $L\alpha$ and $L\beta$ lines of transition metals measured with an X-ray fluorescence spectrometer are explained. Contributions from Coster-Kronig type Auger transition and self-absorption are discussed. Using the $L\beta/L\alpha$ intensity ratio, we can characterize the bond covalency of compounds.

1. Introduction

It is not difficult to measure high-resolution spectra of transition-metal $L\alpha$ and $L\beta$ lines using a conventional X-ray fluorescence spectrometer. Figure 1 [1] shows a typical example of copper $L\alpha, \beta$ spectra of various copper alloys, measured with a RIGAKU 3070 X-ray fluorescence spectrometer equipped with an end window Rh anode X-ray tube (operated at 50 kV and 50 mA). The analyzing crystal was TAP(100) flat crystal ($2d=25.76 \text{ \AA}$). The 2θ scan range was from 58° to 66° by 0.02° steps. The dwelling time for one channel was 5s. The spectra were normalized with respect to the $L\alpha$ maximum. Thirty minutes were enough for the measurement of $L\alpha, \beta$ region with enough signal intensity.

It is found from this Fig. 1 that the intensity of $L\beta$ relative to that of $L\alpha$ is varied from the top to bottom, where the spectra are displayed as the ordering of the copper concentration from lower (silver copper) to 100% (copper).

The $L\alpha$ and $L\beta$ lines are composed of several electric dipole transitions as is shown in Fig. 2. The decay rates for Kr ($Z=36$) calculated by Scofield [2] are listed in Table 1. Assuming that the L_2 and L_3 ionization probability is proportional to the number of electrons, i.e., multiplicity of the core hole states, $L_2/L_3=1/2$, we obtain the X-ray intensity ratio from Table 1 as,

$$\begin{aligned} L_3-M_5(L\alpha_1): L_3-M_4(L\alpha_2): L_2-M_4(L\beta_1): \\ L_2-N_1:L_3-N_1 \\ = 8.88: 1.00: 5.09: 0.02: 0.05. \quad (1) \end{aligned}$$

The exact intensity ratio is $L\alpha_1: L\alpha_2: L\beta_1=9: 1: 5$ if we assume the intensity ratio is proportional to the multiplicity of the state [3]. Comparing these ratios with those of the expression (1), the agreement is satisfactory, and thus the multiplicity is a good approximation to estimate the intensity ratio, in other words, the hole is statistically distributed in each multiplet. Here we use the radiative decay rate for closed shell Kr, because an open 3d shell may affect the transition probability through a spin-spin coupling. The ratio 9: 1 : 5 for closed shell element is a starting point to discuss the intensity ratio of $L\beta/L\alpha$.

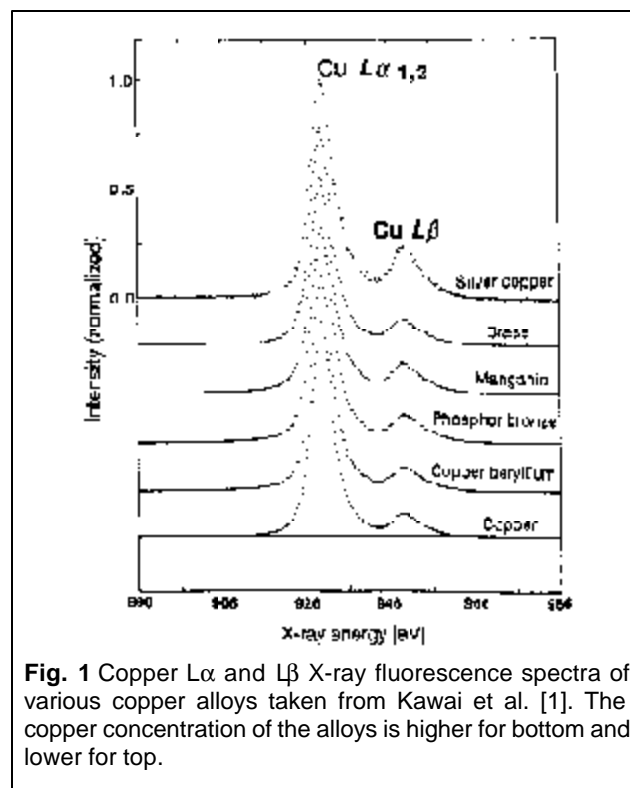


Fig. 1 Copper $L\alpha$ and $L\beta$ X-ray fluorescence spectra of various copper alloys taken from Kawai et al. [1]. The copper concentration of the alloys is higher for bottom and lower for top.

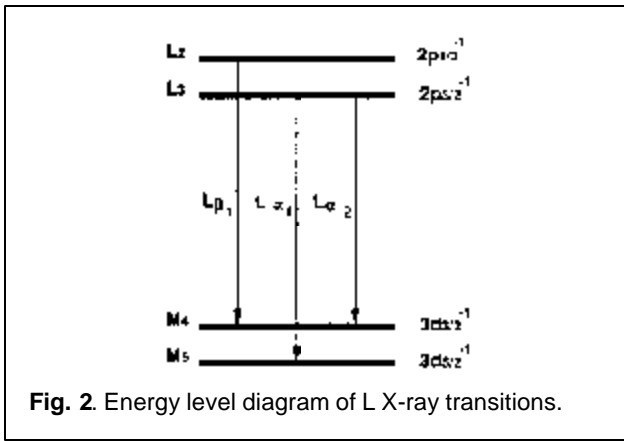


Fig. 2. Energy level diagram of L X-ray transitions.

Table 1 Radiative decay rates of Kr calculated by Scofield [2]

Radiative decay mode	Radiative decay rate [eV/ħ]
L ₂ -M ₄ (Lβ ₁)	0.0237
L ₂ -N ₁	0.00011
L ₃ -M ₄ (Lα ₁)	0.00233
L ₃ -M ₅ (Lα ₂)	0.0207
L ₃ -N ₁	0.00012

The 3d spin-orbit splitting (3d_{3/2} and 3d_{5/2}) is smaller than the spectrometer resolution; we cannot observe Lα₁ and Lα₂ separately for transition metals. Consequently the intensity ratio of Lβ/Lα equals 1/2.

The chemical effects of Lα and Lβ X-ray fluorescence spectra are (i) peak shift, (ii) Iβ/Lα intensity ratio, (iii) profile change, and (iv) line width change. The transition metal Lα and Lβ lines correspond to 2p_{3/2} and 2p_{1/2} lines in X-ray photoelectron spectroscopy (XPS), L₃ and L₂ absorption edges in X-ray absorption near edge structure (XANES), L_{2,3}MM Auger peaks in Auger electron spectroscopy (AES). The binding energy of 2p electrons is from 450 (Ti) to 950 eV (Cu) for transition metals.

Since from the expression (1),

$$L_{2,3}(2p^{-1})-M_{4,5}(3d^{-1}): L_{2,3}(2p^{-1})-N,(4s^{-1}) = 15: 0.1, \quad (2)$$

the 2p⁻¹→4s⁻¹ transition intensity is less than 1% of 2p⁻¹→3d⁻¹ transition.

2. Coster-Kronig Transition

We sometimes tend to think that 3d→2p_{1/2} electric dipole transition (i.e. Lβ emission) takes place after

Table 2 Fluorescent and Coster-Kronig yields of Cu [4].

ω _K	ω ₁	ω ₂	ω ₃	f ₁	f _{1,2}	f _{1,3}	f _{1,3}	f _{2,3}
0.440	0.0016	0.010	0.011	0.839	0.30	0.54	0.000026	0.028

the creation of the L₂ hole by photoionization, when we measure the X-ray fluorescence spectra. However, the portion of this process in all the L₂ hole decay processes is very small. Krause [4] tabulated the transition intensity for all elements, and here the ratios for copper are shown in Table 2. The notation ω_K in Table 2 is the fluorescence yield of K hole state. The value 0.44 means that, when we observe 100 events of the decay process of the K hole, 44 events are filled by a 2p or a 3p electron by the electric dipole transition, and consequently a Kα or Kβ X-ray photon is emitted. The rest 56 holes are filled by one of the 2s, 2p, 3s, 3p, 3d or 4s electrons with non-radiative transition, and one extra electron is ionized. This process is called KLL, KLM, or KMM Auger transition. We cannot observe K X-ray fluorescence line in this non-radiative transition.

ω₁, ω₂, and ω₃ in Table 2 are the X-ray fluorescence yield for L₁, L₂, and L₃ hole state, respectively. f_{1,2}, f_{1,3}, and f_{2,3} are L₁→L₂, L₁→L₃, and L₂→L₃ non-radiative electron transition yields; f₁ is the Coster-Kronig transition for L₁ shell and f₁=f_{1,2}+f_{1,3}, f_{1,3} is the electric dipole 2p→2s transition and thus soft X-ray emission may be observed (166 eV photon for copper).

An Auger transition is concerned by three orbitals: when the principal quantum number of the first and the second orbitals are different, it is called an Auger transition; when they are the same, it is called a Coster-Kronig transition. Parenthetically, when the principal quantum number of all the three orbitals are the same, it is specially called a super-Coster-Kronig transition, but one kind of Coster-Kronig transition.

Suppose that when we observe 100 events of 2p_{1/2} hole decay process (L₂ hole state), since ω₂=0.01 from Table 2, only one hole out of 100 is filled by a 3d electron and an Lβ X-ray photon is emitted. Since f_{2,3}=0.028, three holes are filled by an electron from the L₃ sub-shell by the L₂L₃M_{4,5} Coster-Kronig transition as shown in Fig. 3.

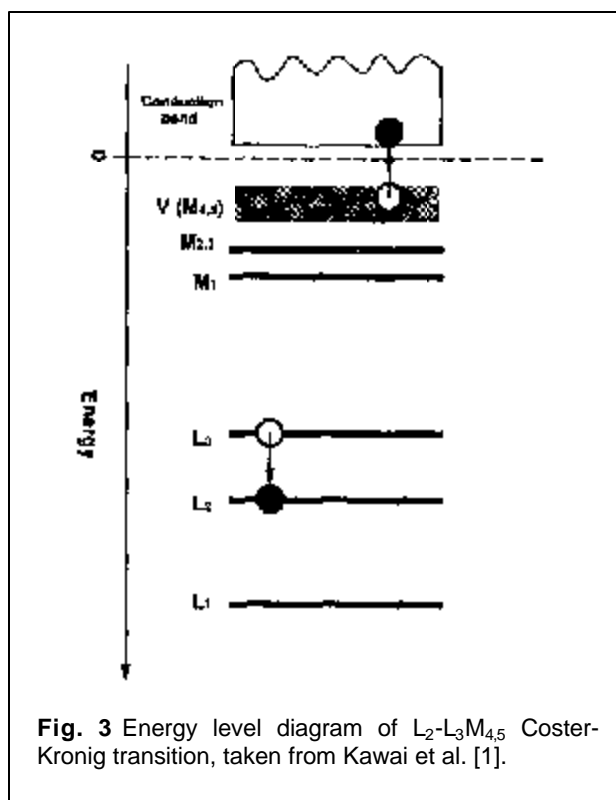


Fig. 3 Energy level diagram of L_2 - $L_3M_{4,5}$ Coster-Kronig transition, taken from Kawai et al. [1].

The binding energy of electrons in Fig. 3 for copper is as follows: 74 eV for $M_{2,3}(3p^{-1})$, 120 eV for $M_1(3s^{-1})$, 931 eV for $L_3(2p_{3/2}^{-1})$, 951 eV for $L_2(2p_{1/2}^{-1})$, and 1097 eV for $L_1(2s^{-1})$. The energy gain in the $L_2L_3M_{4,5}$ Coster-Kronig transition in Fig. 3 is only 20 eV during $L_2 \rightarrow L_3$ transition, thus an electron whose binding energy is less than 20 eV is able to be ionized. The binding energy of the 3p electron is too deep (74 eV), but the 3d or 4s electrons are shallow enough to be ionized. Thus 3 out of 100 L_2 holes are transferred to the L_3 hole state mostly by the $L_2L_3M_{4,5}$ Coster-Kronig transition.

The rest 96 L_2 holes are filled through the L_2MM Auger transition. We can observe strong three tribes of Auger peaks in the XPS wide scan spectra spread over 200 eV, and several peaks in these three tribes are due to this L_2MM Auger transition. The reason that the LMM Auger peaks are visible but LLM Coster-Kronig peaks are invisible in the wide scan XPS spectra is rationalized by the large difference between the LMM and LLM branching ratios, as mentioned above.

Having described the decay process of L_2 hole, we now turn to the decay process of L_1 hole state. If we observe 100 events of 2s ionization (L_1 hole state), 30 holes move to L_2 , 54 move to L_3 since $f_{1,2}=0.30$ and

$f_{1,3}=0.54$ from Table 2. These L_2 and L_3 holes will move again due to the branching ratio as is discussed above. Consequently, though the hole creation probability ratio at photoionization is $L_2/L_3=1/2$, it becomes different from 1/2 just before the X-ray fluorescence. The time required for the LLM Coster-Kronig transition is shorter than the X-ray fluorescence transition. Thus we feel that the $L\beta$ intensity escapes into $L\alpha$ intensity during the measurement of $L\alpha$ and $L\beta$ spectra.

For metals, the binding energy of $M_{4,5}$ shell is shallow, thus $L_2L_3M_{4,5}$ Coster-Kronig transition is energetically possible, as is mentioned above. The deviation from $L\beta/L\alpha=1/2$ for these metallic samples is remarkable as is shown in Fig. 1. These metallic samples show the intensity ratio 1/3, after the correction of the self-absorption effect. The self-absorption correction will be discussed below.

As is mentioned above, the $L_2L_3M_{4,5}$ Coster-Kronig transition is a possible process of modifying the $L\beta/L\alpha$ intensity ratio; this mechanism was pointed out about 40 years ago [5-7]. Recently (after 1985), many applications as well as the electronic structure study using the change of intensity ratio have been reported [8-14].

Other possible process, which modifies the $L\beta/L\alpha$ intensity ratio, is that an L_1 hole is created at first and then the hole moves to L_2 or L_3 shell due to the L_1L_2M or L_1L_3M Coster-Kronig transition. This ratio is 0.30: 0.54 from Table 2, and if this ratio is affected by a chemical environment, a remarkable chemical effect on the $L\beta/L\alpha$ intensity ratio is expected. The ratio $f_{1,2} : f_{1,3} = 0.30 : 0.54$ is approximated by the multiplicity 1 : 2 of the states (L_2 and L_3). The Coster-Kronig ratio $f_{1,2} : f_{2,3}$ is approximately 10: 1. Thus the ratio of the L_1L_2M , L_1L_3M , and $L_2L_3M_{4,5}$ Coster-Kronig transitions are,

$$L_1L_2M : L_1L_3M : L_2L_3M_{4,5} \approx 10 : 20 : 1. \quad (3)$$

Therefore the hole movements within L sub-shells are mostly $L_1 \rightarrow L_2$ or $L_1 \rightarrow L_3$, but not $L_2 \rightarrow L_3$. We must take into account the contribution of the first-created L_1 hole for the explanation of the chemical effect of $L\beta/L\alpha$ intensity ratio.

From the experimental evidence, the $L\beta$ intensity is weaker for small band gap materials, such as metals and covalent compounds, and strong for ionic compounds for Cu. This corresponds to the small or large $M_{4,5}$ binding energy and thus the

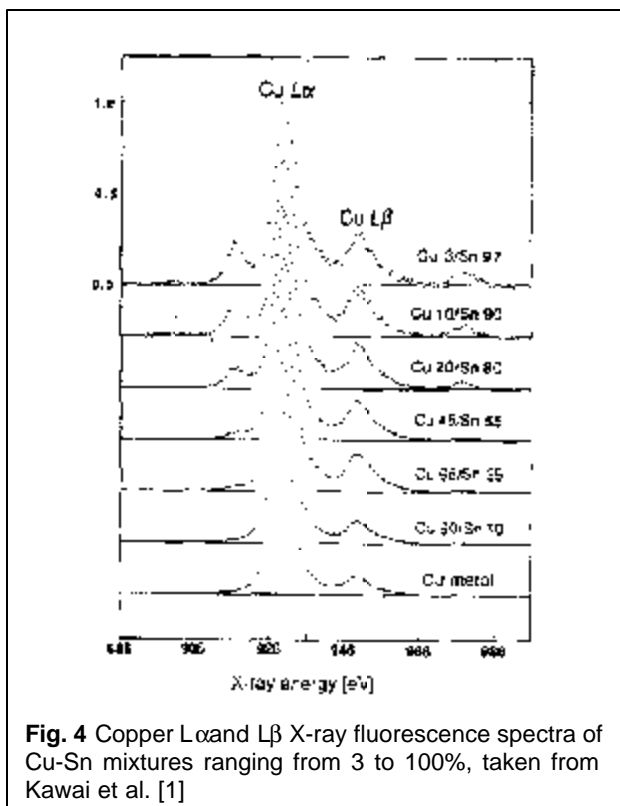


Fig. 4 Copper $L\alpha$ and $L\beta$ X-ray fluorescence spectra of Cu-Sn mixtures ranging from 3 to 100%, taken from Kawai et al. [1]

intensity of $L_2L_3M_{4,5}$ Coster-Kronig transition process. At the present stage, we cannot estimate the chemical effect of the Coster-Kronig transition rate by quantum mechanical calculation; even the order of the transition rate cannot be estimated quantum mechanically.

The energy of the $L\alpha$ emission line after the $L_2L_3M_{4,5}$ Coster-Kronig transition may be slightly different from that of the normal $L\alpha$ X-ray fluorescence. This is because the presence of extra M hole as a spectator, i.e. $L_3M_{4,5} \rightarrow M_{4,5}^2$. The contribution of this extra $M_{4,5}$ hole will be illustrated in nitrogen ion beam excited Ni $L\alpha, \beta$ spectra below (Fig. 7 below).

3. Self-absorption Effect

Figure 4 shows Cu $L\alpha, \beta$ spectra of Cu-Sn alloys [1]. A mixture of Sn and Cu powders were melted in a furnace and rapidly cooled in liquid nitrogen to avoid the atomic diffusion and crystallization. The surfaces of the obtained samples were polished and X-ray fluorescence spectra were measured. The experimental condition of the X-ray fluorescence measurement was similar to that described in the introduction of this review. The smaller the contents of copper, the stronger the $L\beta$ intensity relative to the $L\alpha$ intensity

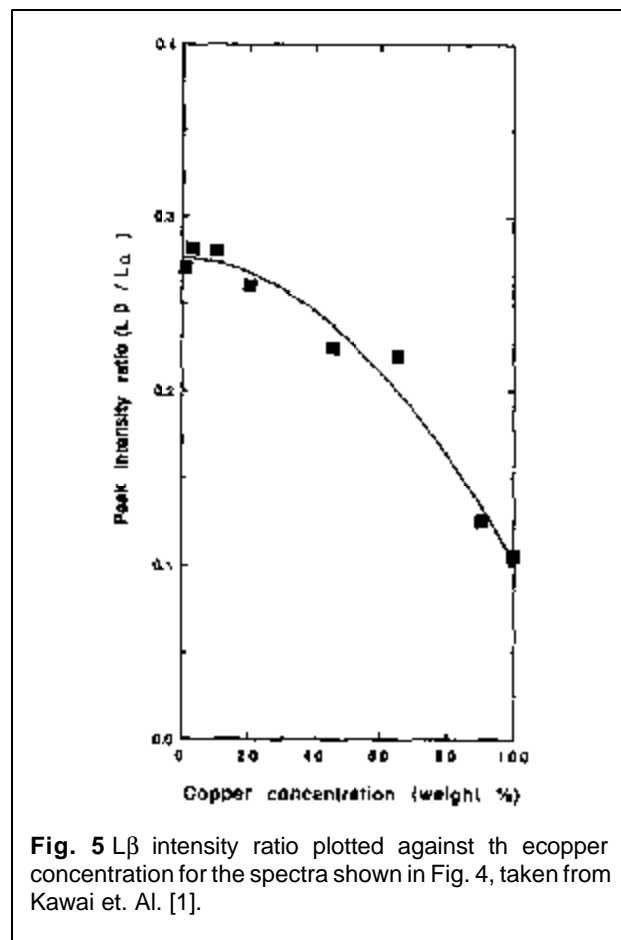
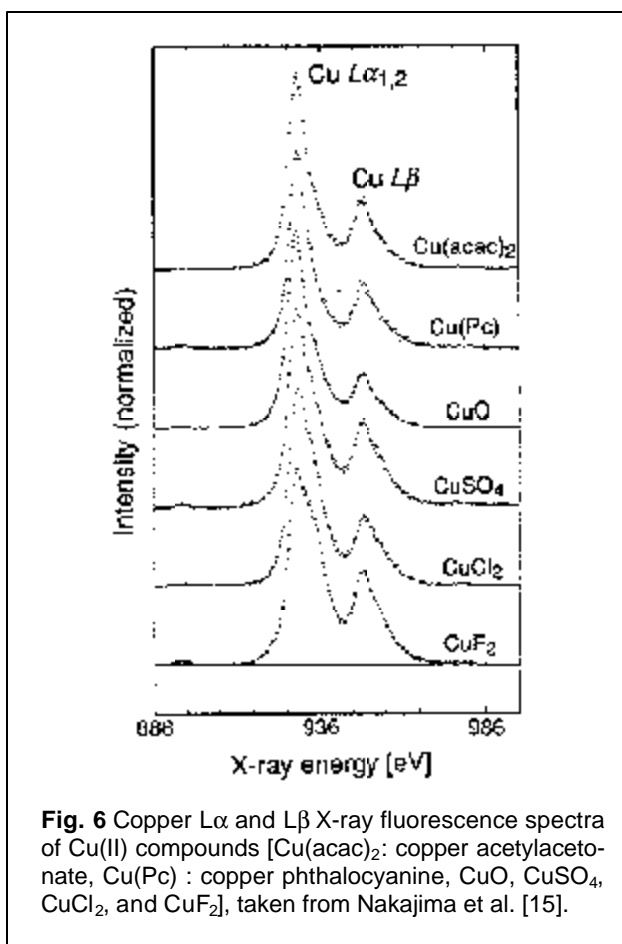


Fig. 5 $L\beta$ intensity ratio plotted against the copper concentration for the spectra shown in Fig. 4, taken from Kawai et al. [1].

becomes. Higher order characteristic lines of Sn are found, but these can be subtracted numerically. Figure 5 is a plot of $L\beta/L\alpha$ intensity ratio against the copper concentration [1]. Here the intensity ratio is the area intensity. The extrapolation of $L\beta$ intensity to the 0% Cu concentration provides us a value 0.28 for the $L\beta/L\alpha$ ratio. This is the true $L\beta$ intensity free from self-absorption effect. This ratio is significantly less than 1/2, which we have discussed above. This difference (0.22) may be due to the Coster-Kronig transition prior to the $L\alpha$ X-ray fluorescence. This ratio becomes close to 1/2 for ionic compounds [CuF_2 , $CuCl_2$, $CuSO_4$, CuO , $Cu(Pc)$, $Cu(acac)_2$] as is shown in Fig. 6 [15]. This may be due to the absence of Coster-Kronig transition for wide band gap compounds.

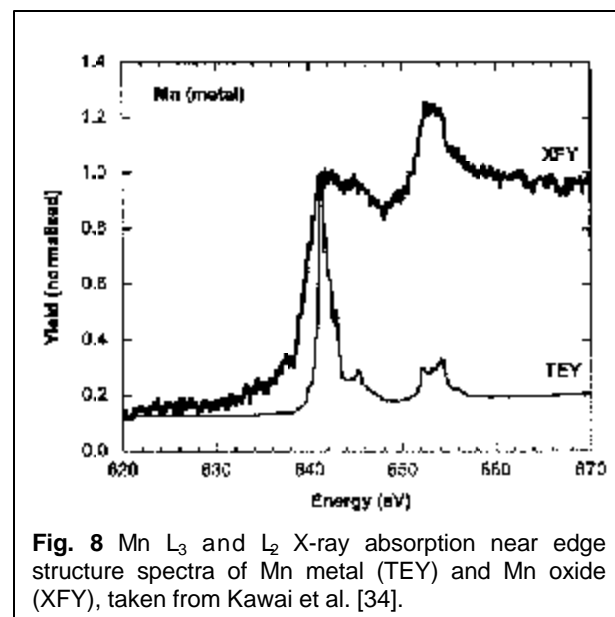
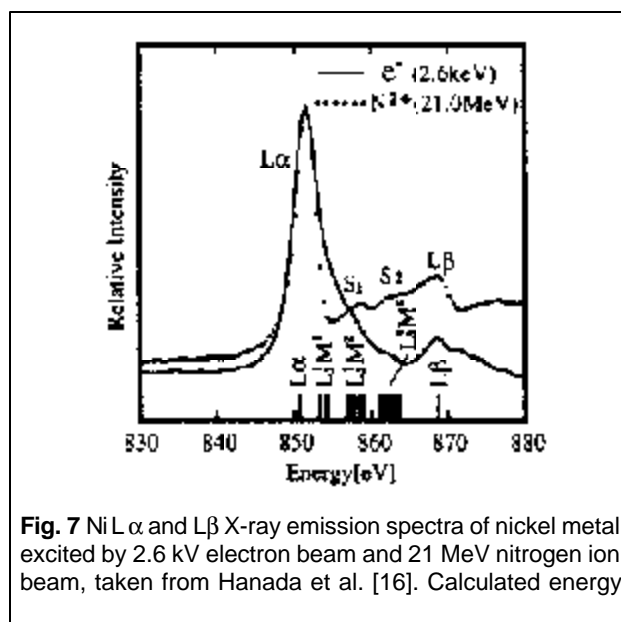
The L_3 and L_2 absorption edges situate at the high energy side of both $L\alpha$ and $L\beta$ lines, respectively. The transition metal fluorescent L X-rays emitted in a solid will be absorbed by another atom of the same element in the solid before they escape from the surface of the solid to the vacuum. A part of the intensity of $L\beta$ is



absorbed by the L_3 edge. The line shape of $L\alpha$ itself is modified by the L_3 absorption edge.

Figure 7 shows nickel metal $L\alpha, \beta$ spectra excited by a 2.6 kV electron beam and a 21 MeV N^{2+} ion beam [16]. High energy nitrogen ions could penetrate into a deep place of the target, and could ionize a 2p electron and additionally several number of M electrons. Thus the ion beam excited spectrum was heavily smeared by the self-absorption effect on the high energy side of $L\alpha$. The line width of $L\alpha$ excited by nitrogen ion is narrower than that excited by an electron beam. The nitrogen excited spectrum shows how the multiple ionization (L_3M_1 , L_3M_2 and L_3M_3) shifts the $L\alpha$ peak, as is indicated by S, and S2 in Fig. 7. The 2.6 kV electron is very low energy, and it loses the energy on the surface due to the inelastic electron scattering. Thus the 2.6 kV electron beam only ionize nickel atoms at shallow places from the surface (less than 1 nm).

Wassdahl and coworkers [17-19] have re-reported the multiple ionization effect on the $L\alpha$ line shape. However, two different explanations exist for the



origin of the high-energy hump of $L\alpha$. One is the multiple ionization effect [16-19] and the other is the charge-transfer effect [20-23]. The charge transfer effect well explains the line shape of $K\alpha$ and $K\beta$ X-ray fluorescence profiles of transition-metal compounds which has partially filled 3d orbital [24-26]. However, on the line shape of $L\alpha$, this effect has been disregarded [27], and an open problem is existing [28, 29]; we must quantitatively clarify the contributions of both multiple-ionization and charge-transfer effects.

From Hartree-Fock-Slater calculations of the ground state and a core hole state [30-32], it is found

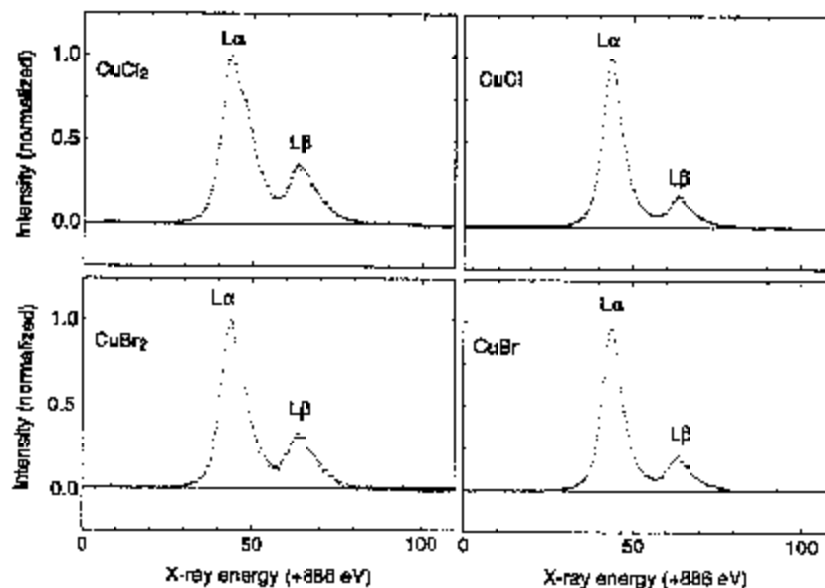


Fig. 9 Measured Cu $L\alpha,\beta$ spectra of divalent and monovalent copper compounds, taken from Kawai et al. [22].

that the charge-transfer effect is important for late transition-metal compounds, but not important for early transition-metal compounds.

We must refer to a famous experiment by Liefeld [33]. He measured Ni $L\alpha,\beta$ X-ray spectra excited at 15 and 2 kV electron beams. He showed that the $L_{2,3}$ X-ray absorption spectra measured for nickel thin foil was identical to the 2 kV spectrum divided by the 15 kV spectrum.

Figure 8 shows Mn metal $L_{2,3}$ absorption spectra measured by the total electron yield (TEY) method and X-ray fluorescence yield (XFY) method [34]. The TEY method is surface sensitive thus this spectrum represents the surface oxide, but the XFY is bulk sensitive, and the XFY spectrum is a metallic spectrum. From this figure, the metallic absorption spectrum has edge jump and its shape is like a step function, and therefore the absorption coefficient at the energy of L_p is still a finite value. However the oxide spectrum has sharp resonance line due to $2p \rightarrow 3d$ absorption. Consequently the absorption coefficients at lower and higher vicinity of L_p line is negligibly small. This holds for other transition metal compounds. Thus the absorption coefficients at the L_p energy position is small and thus the L_p is rather strong for insulators. This is the source of LPILA ratio difference between metallic and ionic compounds. Figure 9 shows spectra of monovalent and divalent copper compounds [22]. The divalent copper compounds have $3d^9$ electron configuration, thus has a

strong $2p \rightarrow 3d$ resonance absorption peak. On the other hand, monovalent copper compounds has $3d^{10}$ electron configuration, thus has step-function-like absorption edge like a metal. Thus the $L\beta$ is more heavily suffered from the self-absorption effect.

Tilting of the sample and the long escape path also smears the L X-ray fluorescence line shape due to the self-absorption effect.

4. Concluding Remarks

Albee et al. [35] reported the Mn and Fe $L\alpha,\beta$ spectra 30 years ago. From their paper, the $L\beta/L\alpha$ intensity ratio becomes greater than 1/2, and this large $L\beta$ has recently reported by Duda et al. [36] for $FeCO_3$ using synchrotron radiation X-ray fluorescence spectroscopy. The $L\beta/L\alpha$ intensity ratio of monovalent copper is less than that of divalent copper. The origin of the change of $L\beta/L\alpha$ intensity ratio may be self-absorption effect or Coster-Kronig transition, or both. We believe that the $L\beta/L\alpha$ intensity is a good index of chemical environment through the self-absorption or Coster-Kronig transition, but we must carefully discriminate these two effects using a "diluent" or tilting the X-ray take-off angle.

References

- [1] J. Kawai, K. Nakajima, and Y. Gohshi, *Spectrochim. Acta* **48B**, 1281 (1993).
- [2] J. H. Scofield, *Phys. Rev.* **179**, 9 (1969).

- [3] E. U. Condon and G. H. Shortley, "The Theory of Atomic Spectra", Cambridge Univ. Press (1935) pp. 322-323.
- [4] M. O. Krause, *J. Phys. Chem. Ref. Data* **8**, 307 (1979).
- [5] H. W. Skinner, T G. Bullen, and J. Jonston, *Philos. Mag.* **45**,1070 (1954).
- [6] J. E. Holliday, *J. Appl. Phys.* **33**, 3259 (1962).
- [7] J. E. Holliday, in "Band Structure Spectroscopy of Metals and Alloys", (Eds.) D. J. Fabian and L. M. Watson, Academic Press, London (1973) p. 713.
- [8] V. R. Galakhov, E. Z. Kurmaev, and V. M. Cherkashenko, *Izv. Akad. Nauk, SSSR, Ser. Fiz.* **49**, 1513 (1985).
- [9] V. R. Galakhov and E. Z. Kurmaev, *Poverhnost (USSR)*, **10**, 107 (1987).
- [10] S. M. Butrin, V. R. Galakhov, E. Z. Kurmaev, and V. I. Glazyrina, *Solid State Commun.* **81**, 1003 (1992).
- [11] E. Z. Kurmaev, A. V. Ezhov, V. M. Cherkashenko, S. N. Shamin, S. Bartkowski, M. Neumann, and A. K. Gangopadhyay, *Solid State Commun.* **105**, 65 (1998).
- [12] E. Z. Kurmaev, V. R. Galakhov, D. A. Zatsepin, V. A. Trofimova, S. Stadler, D. L. Ederer, A. Moewes, M. M. Grush, T. A. Callcott, J. Amtsuno, A. Fujimori, and S. Nagata, *Solid State Commun.* **108**, 235 (1998).
- [13] E. Z. Kurmaev, A. Moewes, V. R. Galakhov, D. L. Ederer, and T Kobayashi, *Nucl. Instrum. Methods Phys. Res.* **B168**, 395 (2000).
- [14] M. V. Yablonskikh, V. I. Grebennikov, Yu. M. Yarmoshenko, E. Z. Kurmaev, S. M. Butrin, L.-C. Duda, C. Sathe, T. Kambre, M. Magnuson, J. Nordgren, S. Plogmann, and M. Neumann, *Solid State Commun.* **117**,79 (2001).
- [15] K. Nakajima, J. Kawai, and Y. Gohshi, *Physica C185-189*, 983 (1991).
- [16] T. Hanada, M. Mogi, J. Kawai, K. Maeda, Y Sasa, and M. Uda, *Nucl. Instrum. Methods Phys. Res.* **B75**, 35 (1993).
- [17] N. Wassdahl, J.-E. Rubensson, G. Bray, P. Glans, P. Bleckert, R. Nyholm, S. Cramm, and N. Mårtensson, *J. Nordgren, Phys. Rev. Lett.* **64**, 2807 (1990).
- [18] N. Wassdahl, Ph. D. Thesis, Uppsala University, Uppsala, Sweden, 1987.
- [19] N. Wassdahl, P. Bleckert, G. Bray, P. Glans, N. Mårtensson, J. Nordgren, J. -E. Rubensson, R. Nyholm, and S. Cramm, 'X-Ray and Inner-Shell Processes', edited by T. A. Carlson, M. O. Krause, and S. T. Manson, AIP Conf. Proc. No. 215, AIP, New York (1 990) pp. 451-464.
- [20] J. Kawai and K. Maeda, *Spectrochim. Acta* **46B**, 1243 (1991).
- [21] J. Kawai and K. Maeda, *Physica C185-189*, 981 (1991).
- [22] J. Kawai, K. Nakajima, K. Maeda, and Y. Gohshi, *Adv. X-Ray Anal.* **35**, 1107 (1992).
- [23] J. Kawai, K. Maeda, K. Nakajima, and Y. Gohshi, *Phys. Rev.* **B48**, 8560 (1993).
- [24] J. Kawai, Y. Nihei, M. Fujinami, Y. Higashi, S. Fukushima, and Y. Gohshi, *Solid State Commun.* **70**, 567 (1989).
- [25] J. Kawai, M. Takami, and C. Satoko, *Phys. Rev. Lett.* **65**, 2193 (1990).
- [26] J. Kawai, C. Suzuki, H. Adachi, T. Konishi, and Y Gohshi, *Phys. Rev.* **B50**, 11347 (1994).
- [27] M. Ohno, *Phys. Rev.* **B52**, 6127 (1995).
- [28] J. Kawai, K. Maeda, K. Nakajima, and Y. Gohshi, *Phys. Rev.* **B52**, 6129 (1995).
- [29] M. Magnuson, N. Wassdahl, and J. Nordgren, *Phys. Rev.* **B56**, 12238 (1997).
- [30] J. Kawai, C. Suzuki, and H. Adachi, *J. Electron Spectrosc. Relat. Phenom.* **78**, 79 (1996).
- [31] C. Suzuki, J. Kawai, Y. Tanizawa, H. Adachi, S. Kawasaki, M. Takano, and T. Mukoyama, *Chem. Phys.* **241**, 17 (1999).
- [32] C. Suzuki, J. Kawai, H. Adachi, and T. Mukoyama, *Chem. Phys.* **247**, 453 (1999).
- [33] R. J. Liefeld, in 'Soft X-ray Band Spectra', Ed. D. J. Fabian, Academic Press, London (1968) pp. 113-149.
- [34] J. Kawai, Y Mizutani, T. Sugimura, M. Sai, T. Higuchi, Y. Harada, Y Ishiwata, A. Fukushima, M. Fujisawa, M. Watanabe, K. Maeda, S. Shin, and Y Gohshi, *Spectrochim. Acta* **B55**,1385 (2000).
- [35] A. L. Albee and A. A. Chodos, *Amer. Miner.* **55**, 491 (1970).
- [36] L.-C. Duda, J. Nordgren, G. Drager, S. Bocharov, and Th. Kirchner, *J. Electron Spectrosc. Relat. Phenom.* **110-111**, 175 (2000).